Self-sensing of deflection, force, and temperature for joule-heated twisted and coiled polymer muscles via electrical impedance

Van Der Weijde, Joost; Smit (student), B.; Fritschi, Michael; Van De Kamp, Cornelis; Vallery, Heike

DOI
10.1109/TMECH.2016.2642588

Publication date
2017

Document Version
Accepted author manuscript

Published in
IEEE - ASME Transactions on Mechatronics

Authors' manuscript. Paper published in IEEE/ASME Transactions on Mechatronics December 2016. Citation information: DOI 10.1109/TMECH.2016.2642588

Self-Sensing of Deflection, Force and Temperature for Joule-Heated Twisted and Coiled Polymer Muscles via Electrical Impedance

Joost van der Weijde, Bram Smit, Michael Fritschi, Cornelis van de Kamp and Heike Vallery

***Abstract*—The recently introduced Twisted and Coiled Polymer Muscle is an inexpensive and lightweight compliant actuator. Incorporation of the muscle in applications that rely on feedback creates the need for deflection and force sensing. In this paper, we explore a sensing principle that does not require any bulky or expensive additional hardware: self-sensing via electrical impedance. To this end, we characterize the relation between electrical impedance on the one hand, and deflection, force and temperature on the other hand, for the Joule-heated version of this muscle. Investigation of the theoretical relations provides potential fit functions that are verified experimentally. Using these fit functions results in an average estimation error of 0.8%, 7.6% and 0.5% for estimating respectively deflection, force and temperature. This indicates the suitability of this self-sensing principle in the Joule-heated Twisted and Coiled Polymer Muscle.**

***Index Terms*—self-sensing, artificial muscle, deflection, inductance, impedance, integrated sensing, compliant actuator**

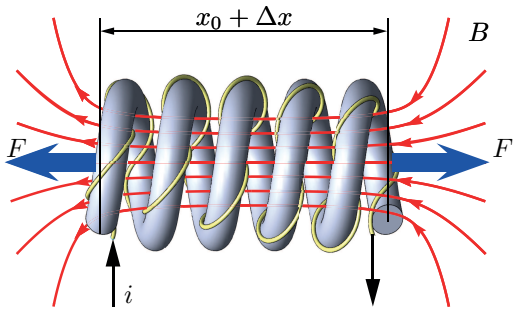

Fig. 1: Electromechanical model of a Joule-heated TCPM. A metal wire wrapped around a polymer helix represents the conductor for Joule heating. The muscle contracts when heated and has a substantial mechanical stiffness, so a force F results from a temperature change or a deflection Δx. The metal wire has an inductance, so a magnetic flux B results from a change in current i through the wire. The wire's resistance changes with temperature. Therefore, the electrical impedance of the muscle provides information on the mechanical state.

I. Introduction

COMPLIANT actuators are a popular area of research [1], [2]. Their inherently low mechanical impedance enables safe interaction with humans, other robots and an uncertain environment. In analogy to the human muscle, often represented by Hill-type models [3], artificial muscles are actuated compliant elements. Polymeric Artificial Muscles (PAMs) form one group within the variety of artificial muscles. Actuators based on Conductive Polymer (CP), Ionic Polymer-Metal Composite (IPMC) and Dielectric Elastomer, amongst others, constitute this group.

Within PAMs, the Twisted and Coiled Polymer Muscle (TCPM) [4] is a recent development. It is a thermally activated actuator in the form of a coil made of a twisted polymer fiber such as a nylon fishing line. Despite low speed and efficiency, this actuator is capable of high strain, high power- and work density [5] and production is inexpensive [4].

Self-sensing actuators are a promising research direction to have truly collocated sensing [6] and to enable closed-loop controlled systems without increasing cost. Dosch and Inman coined the term in 1992 and applied the principle to a piezoelectric actuator [6]. Although a strict definition does not exist, systems are considered self-sensing when information on the state of the system is provided by reading input signal behavior, using a special input signal, or adding additional leads to existing hardware [7]. In general, self-sensing actuators make use of 'smart materials' [8] or 'smart structures' [9].

In PAMs, diverse types of self-sensing already exists: CP actuators consist of a conductive and nonconductive polymer structure placed in an electrolyte. A Faradaic process drives these actuators [10]. Changes in the physical, chemical or thermal domain effectively change the resistivity [7], [11]. A carbon-particle-containing version of this actuator, as presented in [12], works in the same way. IPMC actuators are structures of an ion-conducting polymer membrane coated with metal on either side, placed in deionized water. Ion migration due to application of an electrical potential drives these actuators. The nonuniform ion concentration affects the applied electrical potential [13]. An actuator related to the TCPM is the twisted carbon nanotube yarn actuator. It responds to heat. In [14], a layered version of this actuator measures strain due to changing capacity. In [15], a glucose-containing version of this actuator can sense temperature.

To date, feedback controlled systems with TCPMs still rely on conventional sensing methods for information on their state. Existing applications use encoders [16] and laser distance meters [17] to provide position feedback, and load cells [16] to provide force feedback. Next to these solutions we can imagine the use of linear potentiometers, hall sensors and

Joost van der Weijde, Michael Fritschi, Cornelis van de Kamp and Heike Vallery are with the Robotics Institute of Delft University of Technology, The Netherlands. Please direct correspondence to *j.o.vanderweijde@tudelft.nl*

Part of the research leading to these results has received funding from the SP3-People Programme (Marie Curie Actions) of the European Union's Seventh Framework Programme FP7-PEOPLE-2013-IEF under REA grant agreement n° [627959] and the Marie-Curie career integration grant FP7-PCIG13-GA-2013-618899.

thermocouples to provide feedback when applying TCPMs. The cost of these sensors range from around 1 euro to upwards of 1.000 euro's. Adding the previous solutions to TCPMs increases their weight, size and cost disproportionately. This makes development of self-sensing in TCPMs a priority.

In this paper, we introduce self-sensing for Joule-heated TCPMs. Following up on our work in [18], we make use of the macroscopic resemblance between helical springs and solenoid coils, illustrated in Fig. 1. We characterize a relation between deflection, force and temperature on the one hand and electrical impedance (inductance and resistance) on the other hand. In this first proof of principle, we disregard time-dependent behavior. We evaluate the relation both in theory and in practical experiments, demonstrating usability for sensing.

Section II introduces the TCPM and its production in more detail. Section III contains the derivation of theoretical relations between inductance and resistance on the one hand, and deflection, force and temperature on the other hand. Section IV describes the experiment used to investigate the usability of these relations for sensing. Section V presents the results, followed by the discussion in Section VI and the conclusion in Section VII.

II. The Muscle

This section introduces the working principle of the TCPM, followed by its construction method in general.

A. Working Principle

As explained in [4] two principles form the base of the TCPM's functionality. *i*) A negative thermal expansion in the axial direction, caused by what in rubbers is known as the entropic effect [19]: when heated, highly drawn polymeric fibers access conformational entropy providing reversible contractions. *ii*) Amplification of stroke: inserting twist into the polymer fiber amplifies the tensile stroke. The TCPM is a coil made from this highly twisted fiber. A number of parameters determines the achievable stroke and load capacity, for example: precursor-fiber dimensions and material, number of twists, load while twisting and coil diameter.

Application of heat drives the TCPM. Although a number of methods exist [4], [5], [16], [20], the simplest application oriented method is Joule heating with a resistance wire. Wrapping the resistance wire around the polymer, as illustrated in Fig. 1, distributes contact of the wire with the polymer over the muscle. Passing a current through the resistance wire heats up the wire and subsequently the polymer.

B. Twist Insertion and Incorporation of the Resistance Wire

The construction of the TCPM with Joule heating via a resistance wire follows the method in [4], [17]. We start with aligning a polymer precursor fiber with an equal length of the resistance wire. We jointly clamp one end to a rotational motor. A weight is fixed to the other end using a tether and a system of pulleys, such that it applies a constant load on the fiber under influence of gravity. Rotation of the motor inserts twist. Blocking rotation of the tether prevents the wires from untwisting, while the applied load prevents the wire from snarling. When coils start forming spontaneously (cf. nucleation of coiling or auto coiling [4]), the fiber has reached maximum twist density. At this point we stop twist insertion.

The physical connection between the resistance wire and the polymer fiber has to be reliable in order to achieve repeatable actuation and sensing. As a consequence of the twist insertion process, the resistance wire is automatically wrapped around the thickening polymer fiber and tightened, partly embedding itself in the polymer.

C. Mandrel Coiling and Thermal Annealing

Guiding the resistance-wire-wrapped precursor fiber around a mandrel forms the TCPM. This is done under the same load as the twist insertion process. The ends of the mandrel are manufactured such that the wire's ends line up in the middle of the coil. Mandrel coiling is done such that a homochiral TCPM results [4]. Mandrel formed coils require thermal annealing to retain their shape when taken off the mandrel. Our TCPMs are annealed for one hour at $175\,^{\circ}\mathrm{C}$ in a conventional oven.

D. Training

Training of the muscle is usually seen as repeating the actuation cycle in the setup a number of times before performing the actual experiment [5], [20], [21]. We let muscles undergo a number of cycles of heating and cooling, from room temperature to the maximum actuation temperature, in the intended setup. When the muscle shows repeatable temperature-force behavior, we consider it trained.

III. Self-Sensing Model Derivation

TCPMs could be considered actuated coil springs. Also, TCPMs with Joule heating contain conductive material. Therefore, our reasoning in [18] can be extended to TCPMs: A TCPM's electrical impedance changes with deflection, force and temperature. In a dynamic application, these state variables are highly coupled with each other. Only two are required to fully describe the TCPM's behavior. We assume that in a quasi-static case temperature and deflection are independent, and that force is a function of these two. This section characterizes the dependencies of inductance and resistance on temperature and deflection. We solve the two independent equations to find expressions for deflection and temperature, with inductance and resistance as input. Finally, we find an expression for force dependent on deflection and temperature.

A. Inductance

Several models exist to describe inductance L of coils. The simplest form is

$$L = \mu_0 \frac{N^2}{x} \pi r^2, \tag{1}$$

for example given in [22]. It depends on the magnetic permeability μ_0, the number of windings N, the length x and the radius r of the coil. This equation assumes homogeneity of the magnetic field inside the coil, and it neglects flux leakage.

Adaptations of (1) are introduced in [23], [24] to improve the accuracy of this model. Maxwell provided another approach in [25], by summing the self- and mutual inductances of the individual windings in a coil. Neumann's equation [26] supposedly provides the most accurate model, but requires computation of line- or volume integrals. A more thorough comparison of these inductance theories can be found in [18].

When investigating the relation between coil length and inductance, it becomes apparent that all models show inverse proportional behavior with an offset. In practice, theoretical and actual inductance differ. Recently we showed that a fitting relation with two parameters

$$L\left(\Delta x\right) = \frac{\lambda_x}{\Delta x + x_0} + \lambda_o \tag{2}$$

performs adequately for deflection sensing of coil springs [18]. Herein, Δx is the deflection, and x_0 the known rest length of the spring. The two parameters λ_x and λ_o can be determined using a least-squares fit on minimally two points.

For the metal coil springs of [18], this fit suffices to estimate deflection or force. In the TCPM, however, this fit function does not suffice. Heat drives the system by changing the geometry and properties of the material. A pilot experiment has shown that an increase in temperature gives an offset to the inductance. Therefore, we add temperature T and a parameter λ_T to (2), resulting in

$$L\left(\Delta x, T\right) = \frac{\lambda_x}{\Delta x + x_0} + \lambda_T T + \lambda_o. \tag{3}$$

B. Resistance

An increase in temperature typically increases the resistance of conductors. For the temperature differences under consideration the linear approximation

$$R\left(T\right) = R_0\left(1 + \kappa\left(T - T_0\right)\right) \tag{4}$$

suffices [22]. In this approximation, the actual resistance of the conductor R depends on the resistance R_0 at a known temperature T_0, the current temperature T and the temperature coefficient κ.

Another influence on resistance is deflection of the muscle. This in- or decreases the strain on the Joule-heating wire. Like a common strain gauge, this influences the resistance. A pilot experiment has shown that an increase in deflection, decreases the resistance.

We assume that these influences and possible other influences caused by temperature and deflection are linear and additive. The equation

$$R\left(\Delta x, T\right) = \rho_x \Delta x + \rho_T T + \rho_o, \tag{5}$$

with ρ_x, ρ_T and ρ_o as fitted parameters, describes the dependency of resistance on deflection and temperature.

C. Estimating Temperature, Deflection and Force from Inductance and Resistance

For self-sensing purposes, the above relations for inductance and resistance need to be solved for temperature and deflection. In turn, force depends on both temperature and deflection.

Solving the two independent equations (3) and (5) for their inputs T and Δx gives two nonlinear equations

$$T\left(L, R\right) = \frac{R\lambda_T + L\rho_T - \lambda_T\rho_o - \lambda_o\rho_T + \lambda_T\rho_x x_0 + \sqrt{D}}{2\lambda_T\rho_T}, \tag{6}$$

and

$$\Delta x\left(L, R\right) = \frac{R\lambda_T - L\rho_T - \lambda_T\rho_o + \lambda_o\rho_T - \lambda_T\rho_x x_0 + \sqrt{D}}{2\lambda_T\rho_x}, \tag{7}$$

with

$$\begin{aligned} D = &\left(L\rho_T - R\lambda_T - \lambda_T\rho_x x_0 + \lambda_T\rho_o - \lambda_o\rho_T\right)^2 \\ &+ 4\lambda_x\lambda_T\rho_x\rho_T, \end{aligned} \tag{8}$$

both containing the six presented parameters that need to be identified.

Currently existing models for the TCPM let the force depend linearly on actual deflection and a difference in rest length due to thermal activation [16], [27], [28]. Although cross terms might increase the accuracy of the model, in this paper we chose to follow the linear relation

$$F\left(\Delta x, T\right) = \phi_x \Delta x + \phi_T T + \phi_o, \tag{9}$$

with ϕ_x, ϕ_T and ϕ_o as parameters that need to be identified.

IV. Experiment

This section describes the experiment to validate the fit functions in Section III, including muscle construction, experimental protocol and data analysis.

A. Muscle Construction and Material Choice

The muscle was fabricated according to the method in Sections II-B, II-C and II-D, with the specifications in Table I. A table-mounted drill functioned as the motor. The number of revolutions was counted by an Arduino Uno, reading a hall sensor that was triggered by a permanent magnet attached to the head of the drill. Regarding the precursor fiber, we chose transparent nylon fishing line from *midnight moon* with a diameter of $0.6\,\mathrm{mm}$. The muscle had a rest length after training of $61\,\mathrm{mm}$.

The resistance wire has a dual purpose as it generally serves as the Joule-heating element and here as the probe for self-sensing of temperature, deflection and force. We therefore chose an iron resistance wire with a diameter of $0.2\,\mathrm{mm}$. The temperature coefficient of iron is $\kappa = 6.41 \cdot 10^{-3}\,^{\circ}\mathrm{C}^{-1}$. Equation (4) shows that with a temperature difference of for example $70\,^{\circ}\mathrm{C}$, the resistance should change with an order of magnitude of about 45%.

B. Experimental Setup

Verification of the fit functions required data on temperature, deflection, force, inductance and resistance. Parts of the data were used for fitting, the other parts were used for verification.

We used a *Zwick Z005* Universal Testing Machine (UTM) with heating chamber to control and/or measure temperature,

deflection and force. The heating chamber allowed us to achieve a fully homogeneous temperature distribution in the muscle. The positioning uncertainty of the UTM is $2\,\mu\mathrm{m}$. The uncertainty of the $1\,\mathrm{kN}$ loadcell is 0.35% at 0.2% of its capacity, i.e. an uncertainty of at most $7\,\mathrm{mN}$. The temperature uncertainty of the sensor is $0.5\,^{\circ}\mathrm{C}$.

An LCR43100 by *Wayne Kerr* measured the inductance and resistance via four *RG178B/U* coax cables of $1\,\mathrm{m}$, which allowed for measurements inside the heating chamber. Fig. 2 illustrates the setup and the TCPM in practice.

The measurement-signal frequency of the LCR43100 was based on a pilot experiment. This experiment determined the order of magnitude of resistance and inductance. The signal frequency was set such that the real and imaginary part of the electrical impedance were of approximately the same order of magnitude, with an acceptable measuring uncertainty. With the order of magnitude of resistance and inductance at respectively $10\,\Omega$ and $5\,\mu\mathrm{H}$, a signal frequency of $0.5\,\mathrm{MHz}$ resulted. The relative accuracy of the LCR43100 with this configuration is 0.5%. We neglect a possible influence of the measuring signal on the temperature of the muscle.

C. Protocol

For this experiment, the UTM controlled temperature and deflection, and measured force. A pilot experiment showed that at the conventional maximum actuation temperature of $120\,^{\circ}\mathrm{C}$ [5], [16], [29] and large deflections, the TCPM deformed in an unexpected fashion. Therefore, we chose a uniform temperature distribution with seven points, ranging from $50\,^{\circ}\mathrm{C}$ to $110\,^{\circ}\mathrm{C}$. At each temperature a series of 15 extending and subsequently 15 retracting steps was applied. The deflection ranged from 2 to $30\,\mathrm{mm}$. The UTM extended and retracted at approximately $15\,\mathrm{mm/min}$. Fig. 3 illustrates the sequence of deflection steps, and the division between fitting and verification steps. The UTM logged data at approximately $10\,\mathrm{Hz}$.

The UTM maintained each deflection step for 15 seconds. This allowed the LCR43100 to measure inductance and resistance. A Matlab script was used to time, trigger and read out ten measurements via a serial connection, at each deflection step. A single measurement took approximately 0.8 seconds. The ambient temperature at the start of the experiment was $23\,^{\circ}\mathrm{C}$.

In more detail the protocol was as follows. After training the muscle in the UTM, we calibrated the LCR43100 with the measurement cables connected, to account for their flux area. The trained muscle was then fixed to the top clamp. Suspended from its own weight, the bottom clamp was attached, after which the UTM deflection and force was set to zero. For each reference temperature, the UTM ramped to the temperature, after which the extension/retraction sequence was triggered automatically, and we manually triggered the LCR43100 measuring script. After each sequence the heating chamber was opened and cooled with forced convection for about 5 minutes.

TABLE I: Muscle Construction Specifications

Property	Value
precursor fiber diameter	$0.6\,\mathrm{mm}$
precursor fiber material	nylon
resistance wire diameter	$0.2\,\mathrm{mm}$
resistance wire material	iron
twist per initial fiber length	$\approx$ 400 rotations/m
load at twisting	$\approx 3.00\,\mathrm{N}$
mandrel diameter	$5\,\mathrm{mm}$
mandrel length	$50\,\mathrm{mm}$
annealing temperature	$175\,^{\circ}\mathrm{C}$
annealing time	1 hour
nr. of windings	51
training temperature	$120\,^{\circ}\mathrm{C}$
nr. training cycles	6

D. Data Processing

The LCR43100 provided measurements that relate to a reference deflection at a reference temperature. The UTM provided measurements of temperature, deflection and force related to time. The time intervals where the UTM held its position were indicated by the first and last instants where the deflection deviated less than $1\,\mu\mathrm{m}$ from its reference. Only data within these intervals was used for processing.

The means and standard deviations of all controlled and measured variables were calculated per deflection step. The relative standard deviation was calculated by dividing the absolute standard deviation by the difference between the maximum and minimum mean value of the variable over all data points.

The means and standard deviations provided discretized data points for fitting and verification. The order of the points was based on the moment of measuring. Following this order, the even-numbered mean values were collected in the vectors $\mathbf{R}_f$, $\mathbf{L}_f$, $\mathbf{T}_f$, $\mathbf{\Delta x}_f$ and $\mathbf{F}_f$, and were used for fitting. The odd-numbered mean values were collected in the vectors $\mathbf{R}_v$, $\mathbf{L}_v$, $\mathbf{T}_v$, $\mathbf{\Delta x}_v$ and $\mathbf{F}_v$, and were used for verification. Fig. 3 illustrates this division.

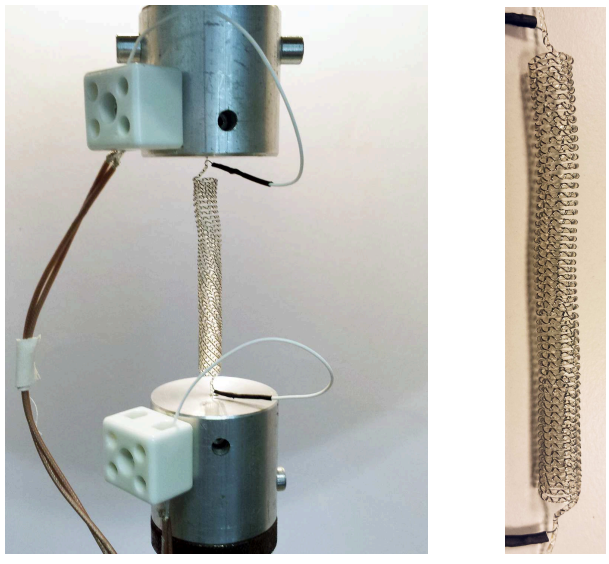

(a) The TCPM in the UTM with four-point measuring cables attached, leading to the LCR43100.

(b) Close-up of the TCPM.

Fig. 2: Illustration of the measurement setup.

E. Data Analysis

The coefficients of (3) and (5) resulted from a least-squares fit, respectively minimizing the errors with respect to the vectors $\mathbf{L}_f$ and $\mathbf{R}_f$, with $\mathbf{\Delta x}_f$ and $\mathbf{T}_f$ as input. We used these coefficients as the initial condition for a nonlinear least-squares optimization with the trust-region-reflective algorithm, to minimize V, given by

$$V = \sum \left(v_1 \left(T(\mathbf{L}_f, \mathbf{R}_f) - \mathbf{T}_f\right)\right)^2 + \left(v_2 \left(\Delta x(\mathbf{L}_f, \mathbf{R}_f) - \mathbf{\Delta x}_f\right)\right)^2, \tag{10}$$

in which the weighing factors $v_1 = {}^1\!/_{110}\,^\circ\mathrm{C}^{-1}$ and $v_2 = {}^1\!/_{30}\,\mathrm{mm}^{-1}$. The coefficients of the fit function for force in (9) were determined by a least-squares fit with the vectors $\mathbf{\Delta x}_f$, $\mathbf{T}_f$, minimizing the error with respect to $\mathbf{F}_f$.

Using the entries of $\mathbf{L}_v$ and $\mathbf{R}_v$ as input for (6) and (7) respectively gave estimates on temperature $\mathbf{T}_e$ and deflection $\mathbf{\Delta x}_e$. These estimates served as an input for (9) to estimate force $\mathbf{F}_e$.

Comparing the estimates $\mathbf{T}_e$, $\mathbf{\Delta x}_e$ and $\mathbf{F}_e$ with the measured values in $\mathbf{T}_v$, $\mathbf{\Delta x}_v$ and $\mathbf{F}_v$ determined the quality of the fit. We used two measures to evaluate the estimation quality. First the R^2 value, or variance explained, measured the quality of fit. It is defined as

$$R^2 = 1 - \frac{\sum_{i=1}^{n}(y_i - f_i)^2}{\sum_{i=1}^{n}(y_i - \bar{y})^2}, \tag{11}$$

in which y_i are the n data points with $\bar{y}$ as their mean, and f_i the estimates. Secondly, the Root Mean Squared Error (RMSE) quantified the estimation error. Comparing the RMSE of the estimates with the standard deviations of the measurements showed the reliability of the fit compared to direct measurements.The relative RMSE was calculated by dividing the absolute RMSE by the difference between the maximum and minimum measured value of the corresponding variable. The relative RMSE illustrated the magnitude of the error compared to the interval of interest.

A fit with predicted isothermal, isometric and isotonic lines illustrated the mapping from inductance and resistance to respectively temperature, deflection and force. The vectors $\mathbf{L}^*$ and $\mathbf{R}^*$ were generated inputs for inductance and resistance. They consisted of fifty equidistant points between the respective minimum and maximum measured values. Equations (6), (7) and (9) provided the outcomes $\mathbf{T}^*$, $\mathbf{\Delta x}^*$ and $\mathbf{F}^*$.

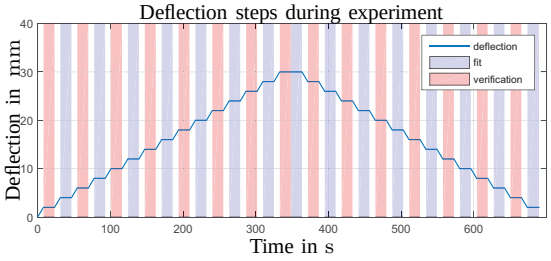

Fig. 3: The deflection steps taken during the experiment for one reference temperature, once the heating chamber had reached that temperature. The blue and red ribbons indicate which data was used for respectively fitting and verification.

V. Results

Table II shows the minimum and maximum measured values of inductance, resistance, temperature, deflection and force. These measurement interval values were used to calculate the relative standard deviations and relative RMSEs. Table II also shows the maximum standard deviations σ for the measured data over all deflection steps and desired temperatures, both as an absolute and a relative value. They indicate the precision of the used instruments and protocol.

Fig. 4a shows the fits for deflection, force and temperature with inductance and resistance as input variables. The dashed lines are the predicted isometric lines of the deflection fit, the solid lines are the predicted isotonic lines of the force fit and the dotted lines are the predicted isothermal lines of the temperature fit. The labels of the iso lines are respectively in mm, N and $^\circ\mathrm{C}$.

Fig. 4b shows the estimated deflection $\mathbf{\Delta x}_e$ at the corresponding measured deflection $\mathbf{\Delta x}_v$. Fig. 4c shows the estimated force $\mathbf{F}_e$ at the corresponding measured force $\mathbf{F}_v$. Fig. 4d shows the estimated temperature $\mathbf{T}_e$ at the corresponding measured temperature $\mathbf{T}_v$. In these figures, the circles indicate the data points for extension and the crosses indicate the data points for retraction. The red solid lines that bisect these figures, indicate the perfect values.

Table III shows the fit-quality measures. Comparing the absolute and relative RMSE to respectively the absolute and relative standard deviations of T, Δx and F in Table II indicates the difference in quality between estimating and measuring these variables.

Table IV shows the fitting parameters for (3) and (5), used in (6), and (7) to respectively estimate temperature and deflection, and the fitting parameters for force in (9).

VI. Discussion

The paper aimed at determining the usability of a static relation between electrical and mechanical properties of a Joule-heated TCPM. This paper took inductance and resistance as the relevant electrical properties to measure, deflection and force as the mechanical state to estimate, and temperature as a relevant intermediate variable. For the investigated TCPM, estimation results showed an RMSE of 0.8% for deflection, 7.6% for force and 0.5% for temperature. More mature sensing solutions for deflection, with a similar range, typically have an uncertainty in the order of magnitude of 0.2%. For existing

TABLE II: Interval of measured inductance, resistance, temperature, deflection and force and the maximum standard deviations σ over a deflection step.

	min	max	σ absolute	σ relative
L	4.254 µH	5.261 µH	0.001 µH	0.1%
R	10.091 Ω	12.083 Ω	0.004 Ω	0.2%
T	50.0 °C	110.0 °C	0.5 °C	0.8%
Δx	2.000 mm	30.000 mm	0.000 mm	0.0%
F	0.05 N	0.79 N	0.01 N	2.0%

TABLE III: Fit quality measures for temperature, deflection and force

	R^2	RMSE absolute	RMSE relative
T	1.000	0.3 °C	0.5%
Δx	0.999	0.23 mm	0.8%
F	0.854	0.06 N	7.6%

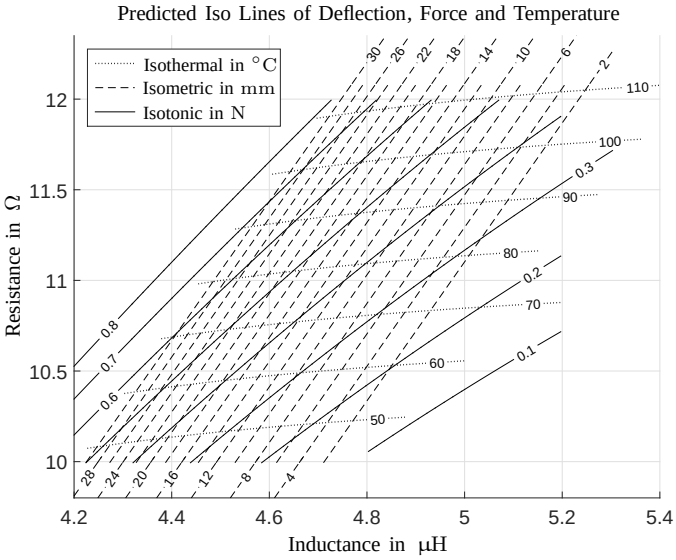

(a) The fit for deflection $\mathbf{\Delta x}^*$, force $\mathbf{F}^*$ and temperature $\mathbf{T}^*$, with inductance $\mathbf{L}^*$ and resistance $\mathbf{R}^*$ as input. The dashed, solid and dotted lines are respectively the predicted isometric, isotonic and isothermal lines of the fit functions. The labels of the iso lines are respectively in mm, N and °C. Please note that, although the experimental conditions are similar, the iso lines are predictions based on the fitted parameters.

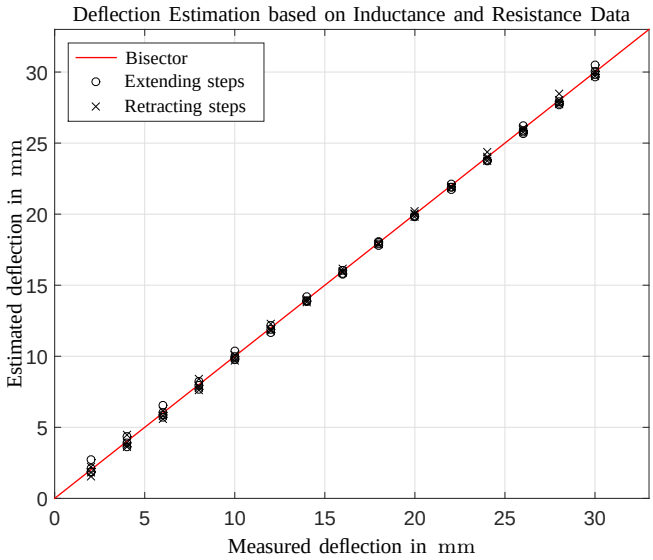

(b) The estimated deflection $\mathbf{\Delta x}_e$, using inductance and resistance as input, versus the measured deflection $\mathbf{\Delta x}_v$. The extending steps are indicated by circles, the retracting steps are indicated by crosses. The solid red bisector indicates the perfect value.

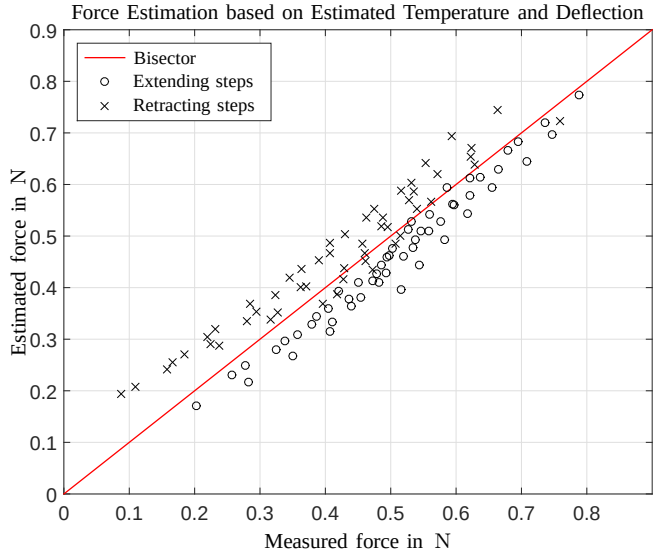

(c) The estimated force $\mathbf{F}_e$, using estimated deflection and temperature as input, versus the measured force $\mathbf{F}_v$. The extending steps are indicated by circles, the retracting steps are indicated by crosses. The solid red line indicates the perfect value.

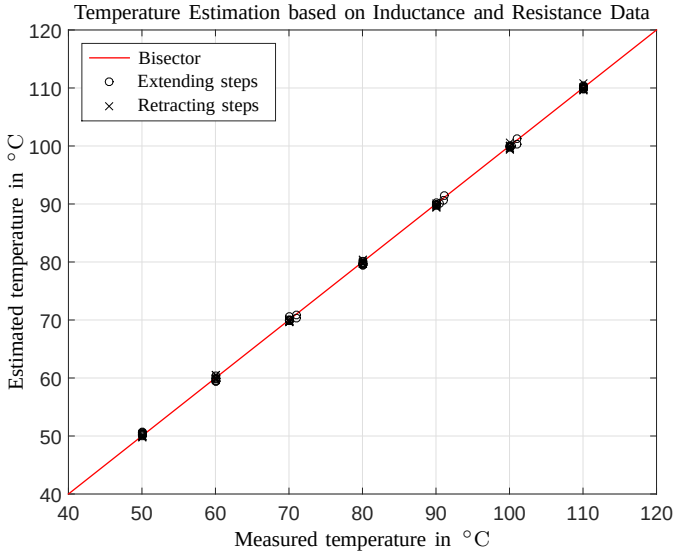

(d) The estimated temperature $\mathbf{T}_e$, using inductance and resistance data as input, versus the measured temperature $\mathbf{T}_v$. The extending steps are indicated by circles, the retracting steps are indicated by crosses. The solid red line indicates the perfect value.

Fig. 4: Graphic representation of fit and verification.

temperature sensors that is typically around 0.5%, and for force also around 0.2%. Compared to these more mature solutions, self-sensing of deflection and temperature already approaches those uncertainties. However, force sensing is still far away from those solutions.

TABLE IV: Fitted parameters for (3), (5) and (9).

$L(\Delta x, T)$		$R(\Delta x, T)$		$F(\Delta x, T)$	
λ_x	107.429 µH.mm	ρ_x	-0.005 Ω/mm	ϕ_x	0.013 N/mm
λ_T	0.008 µH/°C	ρ_T	0.030 Ω/°C	ϕ_T	0.004 N/°C
λ_o	2.670 µH	ρ_o	8.717 Ω	ϕ_o	-0.075 N

Deflection was measured and tracked very accurately, as indicated by the negligible variance. The RMSE can therefore be attributed to the fit function and realization of the muscle.

The slanting of the isometric lines in Fig. 4a shows the influence of temperature on inductance of the muscle. This implies that deflection sensing in TCPM should not rely on inductance only, in contrast to metal coil springs [18].

The RMSE of the force estimate is almost four times the maximum variance within a deflection step. A remarkable feature in Fig. 4c is that the force estimates while extending were generally underestimated and while retracting overesti-

mated. Both might be explained by time-dependent behavior. Although we disregarded it in the fit function descriptions and data processing, in practice we did encounter the effects. Spectral analysis of the force data indicated that frequency content above $2\,\mathrm{Hz}$ had an amplitude lower than the $7\,\mathrm{mN}$ uncertainty of the load cell. For a short analysis of the low frequency behavior, we filtered the force measurements with a $2\,\mathrm{Hz}$ lowpass filter. This revealed a $30\,\mathrm{mN}$ force variation during measurements within a step, which is 4.1% of the force interval. The maximum hysteresis over a full deflection sequence was $149\,\mathrm{mN}$. These values also explain the high variance and RMSE of force estimation.

The variance and RMSE of the estimate of temperature were comparable, so for estimation of temperature the relation with electrical properties is as reliable as a ground truth measurement with a standard temperature sensor. Fig. 4a shows that temperature mainly relates to resistance. However, since resistance also changes with deflection, including inductance in the fit function improves the estimates.

In Fig. 4d some temperature measurements deviate from the reference temperature. The deviations occurred at the initial steps of the respective measurement series. This deviation is due to tracking inaccuracy of the heating chamber. This does not seem to influence the fit.

Implementations of the muscle will involve dynamic behavior. Currently, any damping is disregarded. The estimation principle should therefore be validated in a dynamic setting. Overall, temperature and deflection can be estimated accurately and precisely with a reasonable amount of static parameters. Force estimates should be improved by taking time-dependent behavior into account, for example as in [30]. Moreover, if the application of the TCPM is known, the fit functions could possibly be simplified by including system behavior.

This paper did not investigate the repeatability of these measurements within a muscle, nor did it investigate the repeatability between muscles. Future research towards both will indicate the universality of the fit functions. We expect that the repeatability within a muscle strongly depends on the repeatability of the mechanical behavior of the TCPMs and relates to their time-dependent behavior. This holds particularly for force. Therefore, investigation of this repeatability requires knowledge on creep, relaxation and other time-dependent effects. We expect that the repeatability between muscles strongly depends on the repeatability in production and training. Investigation hereof requires knowledge on the repeatability of production and training.

A more detailed investigation on the influence of deflection and temperature on geometry and properties of the muscle might result in a more appropriate form of the fit function. Future work towards this aspect might improve the universality of the fit functions.

Furthermore, a change in the training procedure, for example training at different loads, might result in a different relation between temperature, deflection and force. This would also affect the universality of the fit. Therefore, future research should also be directed towards the effects of training.

The current work is a proof of principle regarding self-sensing of Joule-heated TCPMs using their electrical impedance. We used a commercially available LCR meter and a heating chamber. When the principle is applied, the characterization should happen under conditions close to their application and with the measurement device used in the application. To that end, future work firstly aims at developing a practical combination of actuation and sensing. Preliminary design indicates that the required electronics for combined actuation and sensing will not exceed the size and cost of available methods. Future work will include a detailed design for such electronics and comparison of its performance to existing sensing solutions for deflection and force. Secondly, future work will combine modeling of the (thermo)dynamic behavior with the presented sensing principle, and validating the static relations in a dynamic setting. Moreover, time-dependent behavior will be included in the fitting relations, likely improving estimation of deflection and force.

VII. Conclusion

In this paper, we introduced self-sensing for Joule-heated TCPMs. We showed that deflection, force and temperature of such a muscle can be estimated with high precision and accuracy from measurements on the system's inductance and resistance. The theoretically derived forms of static relations between the state of the muscle and its electrical impedance were validated by experiments. The relations resulted in an average estimation error of 0.8% for deflection, 7.6% for force and 0.5% for temperature. This paper enables the incorporation of these inexpensive lightweight actuators in applications that require feedback, without the need of expensive sensor hardware.

Acknowledgment

The authors would like to thank Danny de Gans, Ben Schelen, Patrick van Holst and Harry Jansen for their assistance. Finally the authors would like to thank Robert Babuska, Just Herder and Ron van Ostayen for their support.

References

[1] B. Vanderborght, A. Albu-Schaeffer, A. Bicchi, E. Burdet, D. Caldwell, R. Carloni, M. Catalano, O. Eiberger, W. Friedl, G. Ganesh, M. Garabini, M. Grebenstein, G. Grioli, S. Haddadin, H. Hoppner, A. Jafari, M. Laffranchi, D. Lefeber, F. Petit, S. Stramigioli, N. Tsagarakis, M. Van Damme, R. Van Ham, L. Visser, and S. Wolf, "Variable impedance actuators: A review," *Robotics and Autonomous Systems*, vol. 61, no. 12, pp. 1601–1614, dec 2013.

[2] L. Ionov, "Polymeric Actuators," *Langmuir*, vol. 31, no. 18, pp. 5015–5024, nov 2015.

[3] J. M. Winters, "Hill-Based Muscle Models: A Systems Engineering Perspective," in *Multiple Muscle Systems*. New York, NY: Springer, 1990, pp. 69–93.

[4] C. S. Haines, M. D. Lima, N. Li, G. M. Spinks, J. Foroughi, J. D. W. Madden, S. H. Kim, S. Fang, M. Jung de Andrade, F. Göktepe, Ö. Göktepe, S. M. Mirvakili, S. Naficy, X. Lepró, J. Oh, M. E. Kozlov, S. J. Kim, X. Xu, B. J. Swedlove, G. G. Wallace, and R. H. Baughman, "Artificial Muscles from Fishing Line and Sewing Thread," *Science*, vol. 343, no. 6173, 2014.

[5] A. Cherubini, G. Moretti, R. Vertechy, and M. Fontana, "Experimental characterization of thermally-activated artificial muscles based on coiled nylon fishing lines," *AIP Advances*, vol. 5, no. 6, p. 067158, 2015.

[6] J. J. Dosch and D. J. Inman, "Self-Sensing Piezoelectric Actuator for Collocated Control," *Journal of Intelligent Materials Systems and Structures*, vol. 3, no. January, pp. 166–185, 1992.

[7] K. Kruusamä, A. Punning, A. Aabloo, and K. Asaka, "Self-Sensing Ionic Polymer Actuators: A Review," *Actuators*, vol. 4, pp. 17–38, 2015.

[8] M. A. McEvoy and N. Correll, "Materials that couple sensing, actuation, computation, and communication," *Science*, vol. 347, no. 6228, 2015.

[9] H. Janocha, *Adaptronics and Smart Structures*, 2nd ed., H. Janocha, Ed. New York: Springer Berlin Heidelberg, 2007.

[10] D. J. W. Madden, "Conducting Polymer Actuators," Ph.D. dissertation, Massachusetts Institute of Technology, 2000.

[11] T. F. Otero and J. G. Martinez, "Physical and chemical awareness from sensing polymeric artificial muscles . Experiments and modeling," *Progress in Polymer Science*, vol. 44, pp. 62–78, 2015.

[12] H. Tamagawa, W. Lin, K. Kikuchi, and M. Sasaki, "Chemical Bending control of Nafion-based electroactive polymer actuator coated with multi-walled carbon nanotubes," *Sensors & Actuators: B. Chemical*, vol. 156, no. 1, pp. 375–382, 2011.

[13] A. Punning, M. Kruusmaa, and A. Aabloo, "A self-sensing ion conducting polymer metal composite (IPMC) actuator," *Sensors & Actuators: A. Physical*, vol. 136, pp. 656–664, 2007.

[14] Z. F. Liu, S. Fang, F. A. Moura, J. N. Ding, N. Jiang, J. Di, M. Zhang, X. Lepro, D. S. Galvao, C. S. Haines, N. Y. Yuan, S. G. Yin, D. W. Lee, R. Wang, H. Y. Wang, W. Lv, C. Dong, R. C. Zhang, M. J. Chen, Q. Yin, Y. T. Chong, R. Zhang, X. Wang, M. D. Lima, R. Ovalle-Robles, D. Qian, H. Lu, and R. H. Baughman, "Hierarchically buckled sheath-core fibers for superelastic electronics, sensors and muscles," *Science*, vol. 349, no. 6246, pp. 400–404, 2015.

[15] S.-h. Lee, T. H. Kim, M. D. Lima, R. H. Baughman, and S. J. Kim, "Biothermal sensing of a torsional artificial muscle," *Nanoscale*, vol. 8, pp. 3248–3253, 2016.

[16] M. C. Yip and G. Niemeyer, "High-performance robotic muscles from conductive nylon sewing thread," in *2015 IEEE International Conference on Robotics and Automation (ICRA)*. IEEE, may 2015, pp. 2313–2318.

[17] T. Arakawa, K. Takagi, K. Tahara, and K. Asaka, "Position control of fishing line artificial muscles (coiled polymer actuators) from Nylon thread," *Proceedings of SPIE*, vol. 9798, pp. 97 982W–1–97 982W–12, 2016.

[18] J. O. van der Weijde, E. Vlasblom, P. Dobbe, H. Vallery, and M. Fritschi, "Force sensing for compliant actuators using coil spring inductance," in *2015 IEEE/RSJ International Conference on Intelligent Robots and Systems (IROS)*. IEEE, sep 2015, pp. 2692–2697.

[19] C. L. Choy, F. C. Chen, and K. Young, "Negative Thermal Expansion in Oriented Crystalline Polymers," *Journal of Polymer Science*, vol. 19, pp. 335–352, 1981.

[20] S. M. Mirvakili, A. Rafie Ravandi, I. W. Hunter, C. S. Haines, N. Li, J. Foroughi, S. Naficy, G. M. Spinks, R. H. Baughman, and J. D. W. Madden, "Simple and strong: twisted silver painted nylon artificial muscle actuated by Joule heating," in *Proceedings of SPIE, Electroactive Polymer Actuators and Devices*, Y. Bar-Cohen, Ed. International Society for Optics and Photonics, mar 2014, p. 90560I.

[21] S. Aziz, S. Naficy, J. Foroughi, H. R. Brown, and G. M. Spinks, "Characterisation of torsional actuation in highly twisted yarns and fibres," *Polymer Testing*, vol. 46, pp. 88–97, jul 2015.

[22] R. A. Serway and J. W. Jewett, *Physics for Scientists and Engineers*, 9th ed. Brooks/Cole, 2013.

[23] H. Nagaoka, "The Inductance Coefficients of Solenoids," *Journal of the College of Science, Imperial University*, vol. 27, no. 6, pp. 1–33, 1909.

[24] E. B. Rosa, "Calculation of the self-inductance of single-layer coils," pp. 161–187, 1906.

[25] J. Maxwell, "A treatise on electricity and magnetism," London, pp. 1–438, 1873.

[26] D. J. Griffiths, *Introduction To Electrodynamics*, 3rd ed. New Jersey: Prentice Hall, 1999.

[27] S. Kianzad, M. Pandit, A. Bahi, A. Rafie Ravandi, F. Ko, G. M. Spinks, and J. D. W. Madden, "Nylon coil actuator operating temperature range and stiffness," in *Proceedings of SPIE, Electroactive Polymer Actuators and Devices*, Y. Bar-Cohen, Ed. International Society for Optics and Photonics, apr 2015, p. 94301X.

[28] S. Sharafi and G. Li, "A multiscale approach for modeling actuation response of polymeric artificial muscles." *Soft matter*, vol. 11, no. 19, pp. 3833–3843, may 2015.

[29] L. Wu, M. Jung de Andrade, R. S. Rome, C. Haines, M. D. Lima, R. H. Baughman, and Y. Tadesse, "Nylon-muscle-actuated robotic finger," in *Proceedings of SPIE, Active and Passive Smart Structures and Integrated Systems*, W.-H. Liao, Ed. International Society for Optics and Photonics, apr 2015, p. 94310I.

[30] F. Parietti, G. Baud-Bovy, E. Gatti, R. Riener, L. Guzzella, and H. Vallery, "Series Viscoelastic Actuators Can Match Human Force Perception," *IEEE/ASME Transactions on Mechatronics*, vol. 16, no. 5, pp. 853–860, oct 2011.

Joost van der Weijde received a B.Sc. degree in Mechanical Engineering from Delft University of Technology (TU Delft), in Delft, the Netherlands, in 2012. He pursued the M.Sc. degree in Mechanical Engineering at the same university, which he received in 2014. He is currently working toward the Ph.D. degree at the TU Delft Robotics Institute. His research interests include compliant actuation, self-sensing and bipedal locomotion.

Bram Smit received a B.Sc. degree in Mechanical Engineering from Delft University of Technology (TU Delft), in Delft, the Netherlands, in 2014. He pursued the M.Sc. degree in Mechanical Engineering at the same university, which he received in 2016. His research interests lie in the field of biomechanics and modelling.

Michael Fritschi obtained his Dipl.-Ing. in aerospace engineering in 2002 from University of Stuttgart, and his Dr.-Ing. from Bielefeld University in 2016. Previous appointments included the Technical University of Munich, Max-Planck Institute for Biological Cybernetics in Tübingen, IAV GmbH, and Khalifa University, Abu Dhabi. Today, he is a postdoctoral researcher at TU Delft. His research interests include mechatronic design, control, and haptics, applied to robotics and healthcare.

Cornelis van de Kamp received his PhD in Human Movement Science at the Faculty of Medical Sciences, University of Groningen, The Netherlands, in 2011. His research focuses on (human) motor control. Through his Marie Curie Fellowship at the Delft University of Technology, Delft, the Netherlands, he started working on the concept of physiological mechatronics, to eventually aid technologies for health.

Heike Vallery received the Dipl.-Ing. degree in mechanical engineering from RWTH Aachen University, Aachen, Germany, in 2004 and the Doctoral degree from the Technical University of Munich, Munich, Germany, in 2009. She is currently an Associate Professor at the Delft University of Technology, Delft, the Netherlands. Her research interests include the areas of bipedal locomotion, compliant actuation, and rehabilitation robotics.